

Light-polarization dynamics in surface-emitting semiconductor lasers

M. San Miguel,* Q. Feng, and J. V. Moloney

Department of Mathematics, University of Arizona, Tucson, Arizona 85721

(Received 12 January 1995)

A four-level model which takes account of the polarization of the laser field by including the spin sublevels of the conduction and valence bands of a semiconductor allows us to introduce vector rate equations which account for the polarization degree of freedom of the laser emission. Analysis of these rate equations and their extension to include transverse degrees of freedom provides important physical insight into the nature of polarization instabilities in surface-emitting semiconductor lasers. In the absence of transverse effects the model predicts a marginally stable linearly polarized state. The type of dynamical response of the polarization degrees of freedom is linked to the relative time scale of spontaneous-emission and spin-relaxation processes. With transverse effects included, we predict the existence of stable transverse spatially homogeneous intensity outputs with arbitrary direction of linear polarization in the transverse plane. The stability of the off-axis emission solutions to long-wavelength perturbations is investigated and, in addition to an Eckhaus instability associated with a global phase, we predict a polarization instability associated with a relative phase of the complex field vector. The role of phase anisotropy in the laser cavity is explored close to threshold and we predict that it stabilizes two preferred orthogonal directions of polarization, which, however, are discriminated in their stability properties by transverse effects.

PACS number(s): 42.55.Px

I. INTRODUCTION

The basic modeling of semiconductor laser dynamics is provided by rate equations and their generalization to include the dynamics of the phase of the electric field [1]. In spite of the limitations of this model, in particular to describe phenomena involving very short time scales [2], it has been very useful in both basic and applied research in semiconductor laser devices, providing a reference framework for elaborating on more detailed aspects where necessary. However, no such laser modeling seems to be available to describe the polarization properties of the electric field. The rate equations take for granted a fixed direction of polarization. Semiconductor lasers are known to preferentially emit linearly polarized light. This is commonly attributed to cavity anisotropies, but the origin of linearly polarized light has not been considered in detail. On the other hand, it is known for gas lasers that the state of polarization of laser light is linked, in addition of cavity anisotropies, to details of the atomic transitions involved, so that a gas laser can emit linearly or circularly polarized light [3-7]. Phenomena such as polarization switching were studied extensively in the early days of laser physics [3,4,8]. A purpose of this paper is to introduce and analyze a basic model of semiconductor dynamics in which the key aspects of polarization dynamics of a semiconductor laser can be studied. An immediate motivation for our work is that a

number of polarization-sensitive applications of semiconductor laser devices require detailed polarization control [9,10]. The engineering of this polarization control would benefit from a basic modeling of the key physical issues involved. In particular, surface emitting lasers are known to emit linearly polarized light with a polarization stability that is smaller than that for edge emitting lasers. The linear polarization either is randomly oriented in the plane of the active region or prefers two orthogonal directions associated with crystalline orientation [11,12]. Both polarization coexistence between orthogonal modes (polarization mode partition) and polarization switching have been observed [11,12].

A possible justification of the standard rate equations is a two-level model approximation to the semiconductor laser transition. The semiconductor laser is inhomogeneously broadened with different transitions from the conduction to the valence bands for different carrier wave numbers. The two-level approximation can be understood as replacing this transition by a homogeneously broadened transition at the center of the band gap from the conduction to the valence band. The well-known α factor of semiconductor lasers [13] is a common way of summarizing in a parameter many microscopic processes and in particular the inhomogeneously broadened character of the lasing transition. A main effect of the α factor is to produce phase-sensitive dynamics. This sensitivity is analogous to the effect of cavity detuning in two-level models. A useful way to mimic a constant α factor in a two-level approximation to the semiconductor dynamics is to introduce it as a large positive detuning between the cavity frequency and band-gap frequency [14]. Along these lines we will introduce here a four-level model that takes into account the spin sublevels of the conduction and the valence band and therefore allows us to consider

*Permanent address: Departament de Física, Universitat de les Illes Balears, E-07071 Palma de Mallorca, Spain.

different polarizations of light associated with transitions between different spin sublevels. Generalized rate equations that include polarization degrees of freedom are obtained from the four-level model.

The polarization dynamics is closely interrelated with transverse effects in lasers with large Fresnel number. In particular, vertical cavity surface-emitting lasers (VCSEL's) have a well selected single longitudinal mode but can support a large number of transverse modes. It has been observed that different polarization directions are often associated with different transverse modes and/or different emission frequencies [12]. With this motivation, and in order to study general issues of the coupling of polarization and transverse degrees of freedom, we have included in our four-level rate equations a general modeling of transverse effects for broad area lasers. Our study is based on a one-dimensional transverse structure with free boundaries. It follows the same spirit as other analyses [15–17] aiming an understanding of intrinsic bulk dynamical effects in broad area lasers. A direct comparison of our results with polarization dynamics coupled with transverse effects in VCSEL's requires further investigation taking into account a finite-size two-dimensional geometry and possible index-guiding effects. Previous studies of the dynamics of transverse effects in broad area semiconductor lasers [16,18], feature either mean-field equations obtained by averaging of the longitudinal spatial degrees of freedom or full counterpropagating wave simulations. Mean-field equations can be seen as rate equations supplemented with diffraction terms for the field and diffusion terms for the carriers. They predict that the transverse spatially homogeneous lasing solution is unstable. However, they also include an unphysical instability at high transverse wave numbers, which in the context of two-level models can be traced back to adiabatic elimination of the dipole polarization variables [17]. We depart here from this approach and, instead of an adiabatic elimination of the dipole polarization variables, we introduce, close to threshold, an amplitude equation description of the broad area semiconductor laser dynamics. The main idea of this alternative approach is the same as that used for the study of transverse effects of two-level models of wide gain gas lasers [15]. In our case this description, on the one hand, identifies the preferred transverse mode of laser emission and, on the other hand, includes the light polarization degrees of freedom. A similar amplitude equation approach to polarization dynamics together with transverse effects has been recently given for some gas lasers [19].

The basic four-level model introduced in Sec. II accounts for the vector nature of the laser emission field by allowing for both states of circular polarization through dipole-allowed transitions between independent pairs of levels. Coupling between both transitions is assumed to occur via spin-flip relaxation processes [20–24]. Section III details a rate equation analysis of the coupled system where the polarization dynamics has been adiabatically eliminated. The relative time scales of spontaneous emission and spin-flip relaxation processes is shown to be of critical importance in determining the nature of the polarization dynamics and the stability of the linearly po-

larized laser light field.

The inclusion of transverse degrees of freedom in Sec. IV significantly increases the set of allowed lasing emission states. Off-axis far-field homogeneous intensity linearly polarized solutions corresponding to near-field traveling waves with an arbitrary direction of linear polarization are shown to be linearly stable. A different class of linearly stable states consisting of a superposition of traveling waves with opposite senses of circular polarization manifest themselves as a periodic alternation in the direction of linear polarization in the transverse plane. Many of the allowed transverse lasing solutions are shown to be either intrinsically unstable over physically realistic parameter ranges or susceptible to long-wavelength instabilities of the global or relative phase. The latter defines the polarization state of the laser field while the former reflects translational invariance in the transverse plane. The role of carrier diffusion as well as light diffraction on the stability of the various laser-emission solutions is explicitly taken into account. Anisotropies in the laser cavity and their interplay with transverse effects are discussed in Sec. V within the reduced description valid close to threshold. Linear phase anisotropies associated with birefringence stabilize two preferred orthogonal directions for off-axis linearly polarized emission. An important conclusion of this section is, however, that transverse effects discriminate between these two preferred directions so that, for a given sign of the anisotropy, they extend the range of stability to transverse perturbations of the x -polarized solution while the y -polarized stability range shrinks.

II. A FOUR-LEVEL MODEL FOR POLARIZATION DYNAMICS OF QUANTUM-WELL LASERS

The polarization of laser light is of quantum nature and it originates in the spin sublevels of the lasing transition between the conduction and valence bands of the semiconductor. The band structure near the band gap can be calculated using the Luttinger Hamiltonian and $\mathbf{k} \cdot \mathbf{p}$ theory [25]. The electron state of zero momentum of the conduction band has a total angular momentum $J = 1/2$. The valence bands are commonly known as heavy hole (hh), light hole (lh), and split-off (so). When taking into account spin-orbit coupling, the so band, which with angular momentum $J = 1/2$, has a lower energy than the hh and lh bands and it can be disregarded for our purposes. For bulk material the hh and the lh bands are degenerate at the center of the band gap with a total angular momentum $J = 3/2$. For quantum wells, the quantum confinement in the z direction removes this degeneracy. In the case of unstrained quantum wells, the heavy-hole band, which is associated with $J_z = \pm 3/2$, has a higher energy (Fig. 1). We will consider a surface-emitting quantum-well laser so that the active material slab is perpendicular to the direction of laser emission z , which coincides with the quantization axis (Fig. 2). In this geometry and for a gain-guided broad area laser the electric field is in the x - y plane, so that two independent

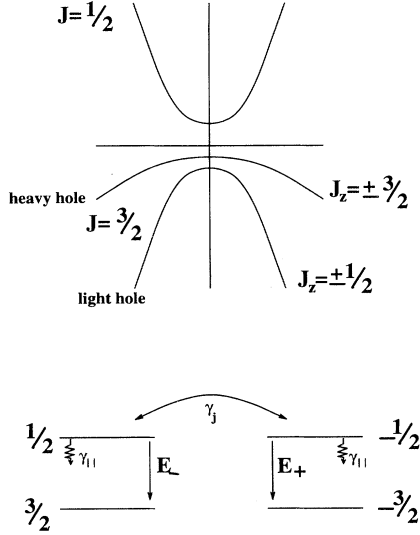


FIG. 1. Band structure of a quantum well.

TE polarization modes are available for the laser field. For such a transverse electric field the allowed dipole transitions are those in which $\Delta J_z = \pm 1$. Right circularly polarized light corresponds to $\Delta J_z = -1$ and left circularly polarized light to $\Delta J_z = +1$. Given the lower energy of the light-hole band we will neglect transitions from the conduction to the light-hole band. We are then left with two allowed transitions between the conduction and the heavy-hole band: the transition from $J_z = -1/2$ to $J_z = -3/2$ associated with right circularly polarized light and the transition from $J_z = 1/2$ to $J_z = 3/2$ associated with left circularly polarized light. In a first approximation to semiconductor polarization dynamics, we can model these transitions by the four-level model depicted in Fig. 1. We write the vector electric field for a single longitudinal mode laser as

$$\mathbf{E} = [F_x(x, y, t)\hat{\mathbf{x}} + F_y(x, y, t)\hat{\mathbf{y}}] e^{iKz - i\nu t} + \text{c.c.}, \quad (2.1)$$

The slowly varying amplitudes F_x, F_y satisfy the Maxwell-Bloch equations [26], which are conveniently written in terms of the right and left circularly polarized

components

$$F_{\pm} = \frac{1}{\sqrt{2}}(F_x \pm iF_y). \quad (2.2)$$

The Maxwell-Bloch equations are

$$\partial_t F_{\pm} = -\kappa F_{\pm} - ig_0^* P_{\pm} + i \frac{c^2}{2\nu} \nabla_{\perp}^2 F_{\pm}, \quad (2.3)$$

$$\partial_t P_{\pm} = -[\gamma_{\perp} + i(\omega - \nu)] P_{\pm} + ig_0 F_{\pm} (D \pm d), \quad (2.4)$$

$$\partial_t D = -\gamma_{\parallel} (D - \sigma) + [ig_0^* (F_+^* P_+ + F_-^* P_-) + \text{c.c.}] + D_f \nabla_{\perp}^2 D, \quad (2.5)$$

$$\partial_t d = -\gamma_J d + [ig_0^* (F_+^* P_+ - F_-^* P_-) + \text{c.c.}] + D_f \nabla_{\perp}^2 d. \quad (2.6)$$

F_{\pm} are associated with the transitions $\mp 1/2 \rightarrow \mp 3/2$, respectively. P_{\pm} are the slowly varying amplitudes of the dipole polarizations associated with these transitions. The population differences D and d are defined as

$$D = \frac{1}{2}[(n_1 + n_{-1}) - (n_3 + n_{-3})], \quad (2.7)$$

$$d = \frac{1}{2}[(n_{-1} - n_{-3}) - (n_1 - n_3)], \quad (2.8)$$

where n_i is the population of the spin sublevel $i/2$. D is associated with the total population difference between the conduction and the valence bands and d is associated with the difference in population inversions associated with right and left circularly polarized emissions. The coupling between the two lasing transitions occurs through nonzero values of d . Density-matrix coherences other than the two dipole polarizations P_{\pm} are decoupled from Eqs. (2.3)–(2.6) and will not be considered any further. The model also includes a transverse diffraction term and carrier diffusion [$\nabla_{\perp} = (\partial_x, \partial_y)$]. The parameters in (2.3)–(2.6) are the cavity frequency ν , the frequency ω associated with the energy gap, the coupling constant g_0 , and an incoherent pumping parameter σ associated with the injection current. The model includes several decay rates: κ is the inverse photon lifetime in the cavity and γ_{\perp} the relaxation rate of the dipole polarization. The population difference D has a decay rate γ_{\parallel} associated with spontaneous decay, while d has a decay rate

$$\gamma_J = \gamma_{\parallel} + 2\gamma_j. \quad (2.9)$$

The decay rate γ_j accounts for the mixing of the populations with opposite value of J_z . This parameter is introduced to model spin-flip relaxation processes. For simplicity we assume the same decay rate γ_j in the conduction and the valence bands. Several spin relaxation processes for electrons and holes have been identified in semiconductors [20] as, for example, hole interaction with static scatterers [21] or exchange interaction between electron and hole [22]. These processes are often studied in the context of luminescence phenomena [23] and significant differences in relaxation times between bulk and quantum-well materials are found [23,24]. For our purposes the parameter γ_j can be understood as a phenomenological modeling of a variety of complicated mi-

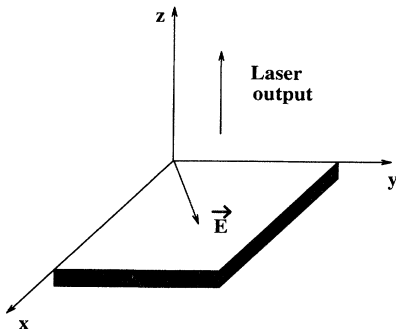


FIG. 2. Geometry of a surface-emitting laser.

crossopic processes. From experimental measurements [24] of spin relaxation times in quantum wells one can estimate that

$$\gamma_{\parallel} \leq \gamma_j \leq 10^2 \gamma_{\parallel}, \quad (2.10)$$

where $\gamma_{\parallel}^{-1} \approx 1$ nsec. The spin mixing described by γ_j typically occurs on larger time scales than photon decay, where $\kappa^{-1} \approx 1$ psec. The fastest time scale included in (2.3)–(2.6) is the dipole polarization decay rate $\gamma_{\perp} \gg \gamma_{\parallel}$. The implications of these differences in time scales will be considered throughout the remainder of the paper.

III. RATE EQUATIONS APPROXIMATION

In this section we analyze a rate equation approximation to describe polarization dynamics of a single longitudinal surface emitting semiconductor laser in cases where transverse effects can be neglected. Given the much faster relaxation rate γ_{\perp} of the dipole polarization variables, they can be adiabatically eliminated:

$$P_{\pm} = \chi_{\pm} F_{\pm} = \frac{g_0(\Omega + i\gamma_{\perp})}{\gamma_{\perp}^2 + \Omega^2} (D \pm d) F_{\pm}, \quad (3.1)$$

where $\Omega = \omega - \nu$ is the detuning. The conventional constant α factor of single-mode semiconductor laser theory [13] is defined in terms of the susceptibilities χ_{\pm} as

$$\frac{\text{Re}\chi_{\pm}}{\text{Im}\chi_{\pm}} = \frac{\Omega}{\gamma_{\perp}} \quad (3.2)$$

and it can be formally identified with a large positive detuning Ω of the four-level model [14].

Replacing (3.1) and (3.2) in (2.2)–(2.5) we find a generalized set of rate equations

$$\partial_t E_{\pm} = -\frac{\kappa}{\gamma_{\perp}} E_{\pm} + \frac{\kappa}{\gamma_{\perp}} (1 - i\alpha)(N \pm n) E_{\pm}, \quad (3.3)$$

$$\begin{aligned} \partial_t N = & -\frac{\gamma_{\parallel}}{\gamma_{\perp}} (N - \sigma/\sigma_c) - (|E_+|^2 + |E_-|^2) N \\ & - (|E_+|^2 - |E_-|^2) n, \end{aligned} \quad (3.4)$$

$$\begin{aligned} \partial_t n = & -\frac{\gamma_J}{\gamma_{\perp}} n - (|E_+|^2 - |E_-|^2) N \\ & - (|E_+|^2 + |E_-|^2) n, \end{aligned} \quad (3.5)$$

where time has been rescaled as $t \rightarrow \gamma_{\perp} t$ and

$$\begin{aligned} E &= \sqrt{2g} F, \quad N = \frac{g\gamma_{\perp}}{\kappa} D, \quad n = \frac{g\gamma_{\perp}}{\kappa} d, \\ \alpha &= \frac{\Omega}{\gamma_{\perp}} = \frac{\omega - \nu}{\gamma_{\perp}}, \quad g = \frac{|g_0|^2}{\gamma_{\perp}^2 + \Omega^2}, \quad \sigma_c = \frac{\kappa}{g\gamma_{\perp}}. \end{aligned}$$

We note that formally taking $n = 0$ and $E_+ = E_-$, (3.3)–(3.5) reduce to the familiar rate equations, where N is the difference between the actual carrier number and the carrier number at transparency.

The rate equations have a cw solution above threshold that corresponds to linearly polarized light:

$$\begin{aligned} E_{\pm} &= Q e^{i\frac{\alpha\kappa}{\gamma_{\perp}} t + i(\theta_0 \pm \psi_0)}, \quad N = 1, \quad n = 0 \\ Q^2 &= \frac{1}{2} \frac{\gamma_{\parallel}}{\gamma_{\perp}} \left(\frac{\sigma}{\sigma_c} - 1 \right), \end{aligned} \quad (3.6)$$

where θ_0 and ψ_0 are arbitrary phases. The global phase θ_0 is the familiar arbitrary phase of conventional theory. The relative phase ψ_0 indicates the arbitrary direction of linear polarization in the transverse plane of the laser.

The linear stability of this solution can be studied by writing

$$\begin{aligned} E_{\pm} &= (Q + a_{\pm}) e^{i\frac{\alpha\kappa}{\gamma_{\perp}} t}, \\ N &= 1 + \Delta, \quad n = \delta. \end{aligned}$$

In terms of $S = a_+ + a_-$ and $R = a_+ - a_-$, the linearized equations decouple into two sets

$$\begin{aligned} \dot{S} &= \frac{2\kappa}{\gamma_{\perp}} (1 - i\alpha) Q \Delta, \\ \dot{\Delta} &= -\frac{\gamma_{\parallel}}{\gamma_{\perp}} \Delta - Q[(S + S^*) + 2\Delta Q]; \end{aligned} \quad (3.7)$$

$$\begin{aligned} \dot{R} &= \frac{2\kappa}{\gamma_{\perp}} (1 - i\alpha) Q \delta, \\ \dot{\delta} &= -\frac{\gamma_J}{\gamma_{\perp}} \delta - Q[(R + R^*) + 2\delta Q]. \end{aligned} \quad (3.8)$$

In a linear analysis, the imaginary part of a_{\pm} is associated with the phase of the perturbation of Q , so that the imaginary part of S is associated with the perturbation of the global phase θ_0 and the imaginary part of R with the relative phase ψ_0 .

The set of equations (3.7) is independent of the coupling γ_j between the transitions $\pm 1/2 \rightarrow \pm 3/2$. This set describes the small signal analysis of the global transition from the conduction to the valence band. It coincides with the small signal analysis of conventional rate equations. There is a zero eigenvalue and two complex eigenvalues (complex conjugate). The only nonvanishing component of the eigenvector corresponding to the zero eigenvalue is the imaginary part of S . Such an eigenvalue reflects the invariance of the equations under time translation or, equivalently, the arbitrary value of the global phase θ_0 of the complex electric field. The complex conjugate eigenvalues describe relaxation oscillations of frequency ω_R . In the usually considered limit $(\frac{\sigma}{\sigma_c})^2 \ll \frac{8\kappa}{\gamma_{\parallel}} (\frac{\sigma}{\sigma_c} - 1)$, the complex eigenvalues are

$$\begin{aligned} \lambda &\simeq -\frac{\gamma_{\parallel}}{2\gamma_{\perp}} \frac{\sigma}{\sigma_c} \pm i\omega_R, \\ \omega_R &= 2 \left(\frac{\kappa}{\gamma_{\perp}} \right)^{1/2} Q. \end{aligned}$$

The second set of equations (3.8) describes the dynamical response associated with the polarization degrees of freedom. There is a zero eigenvalue associated with the imaginary part of R . This eigenvalue reflects the invariance of the equations under rotations of the vector electric field or, equivalently, the arbitrary direction of linear polarization determined by the relative phase ψ_0 . The other two eigenvalues can be real or complex conjugate, but they always have a negative real part, which ensures the stability of the linearly polarized laser light. They describe the relaxation of polarization fluctuations and, when they are complex, they identify relaxation oscil-

lations associated with polarization degrees of freedom. The change from complex to real eigenvalues separates two regimes of dynamical response of the polarization. Each regime exists for a range of values of $\frac{\gamma_J}{\gamma_{||}}$. For $\gamma_J = \gamma_{||}$ ($\gamma_j = 0$) the two transitions $\pm 1/2 \rightarrow \pm 3/2$ are uncoupled, the set of equations for R and δ is degenerate with the set for S and Δ , and the eigenvalues are complex. Increasing $\gamma_J/\gamma_{||}$ from $\gamma_J/\gamma_{||} = 1$, the eigenvalues continue to be complex, with a growing absolute value of the real part, up to a value $(\frac{\gamma_J}{\gamma_{||}})_c$. In this regime the damping rate of the polarization relaxation oscillations grows. For $\gamma_J/\gamma_{||} = (\frac{\gamma_J}{\gamma_{||}})_c$ the two complex conjugate eigenvalues become two real eigenvalues and there is a change of behavior in the dynamical response from relaxation oscillations to exponential relaxation with two real time constants. In the limit $\frac{\gamma_J}{\gamma_{||}} \rightarrow \infty$ one of the real eigenvalues approaches zero. In this limit the linearly polarized emission becomes marginally stable with respect to amplitude fluctuations. The growth of such fluctuations would imply the growth of the real part of R , that is, the suppression of one of the two circularly polarized components of the field, and it would lead to circularly polarized emission (Fig. 3). The value of $(\frac{\gamma_J}{\gamma_{||}})_c$ at which two complex eigenvalues of (3.8) become real is given, for $\frac{8\kappa}{\gamma_{||}} \gg \frac{\sigma - \sigma_c}{\sigma_c}$, as

$$\left(\frac{\gamma_J}{\gamma_{||}}\right)_c \simeq \left(\frac{8\kappa}{\gamma_{||}} \frac{\sigma - \sigma_c}{\sigma_c}\right)^{1/2}. \quad (3.9)$$

For $\frac{\gamma_J}{\gamma_{||}} \gg (\frac{\gamma_J}{\gamma_{||}})_c$ the dominant eigenvalue becomes

$$\lambda = -\frac{8\kappa}{\gamma_{||}} \frac{\sigma - \sigma_c}{\sigma_c} \frac{\gamma_{||}}{\gamma_J}. \quad (3.10)$$

In summary, the dynamical response depends on the relative time scales of spontaneous emission and spin-flip relaxation. When the spin-flip process is fast enough, the relaxation oscillations associated with the polarization degree of freedom disappear and the faster this process becomes, the longer the relaxation time of amplitude polarization fluctuations. The result is that, as the cou-

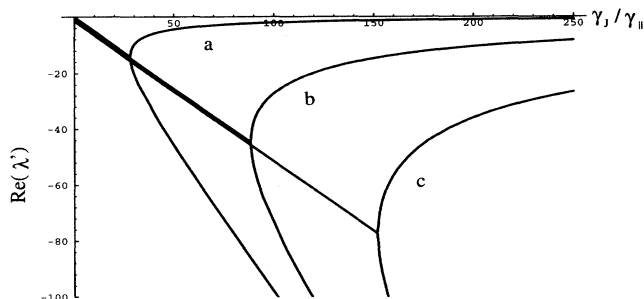


FIG. 3. Real part of the polarization eigenvalue $\lambda' = \lambda/\frac{\gamma_{||}}{\gamma_{\perp}}$ vs $\gamma_J/\gamma_{||}$ for $(\kappa/\gamma_{||}) = 10^3$. The curves correspond to different values of $\frac{\sigma - \sigma_c}{\sigma_c}$: (a) 0.1, (b) 1, and (c) 3.

pling γ_j between the two transitions $\pm 1/2 \rightarrow \pm 3/2$ increases, there is a crossover from well stabilized linearly polarized emission to a poorly stabilized situation with a long relaxation time of the fluctuations away from linearly polarized emission. The relaxation time diverges for $\frac{\gamma_J}{\gamma_{||}} \rightarrow \infty$.

Our previous discussion neglects the effect of spontaneous-emission noise. When taking noise into account the two arbitrary phases θ_0 and ψ_0 diffuse. The diffusion of the global phase θ_0 results in the loss of frequency coherence of the laser and gives rise to the laser linewidth. The diffusion of ψ_0 leads to a random motion of the direction of linear polarization. Both diffusion processes are driven by the same source of noise and occur on the same time scale, which is the coherence time of the laser. This time is estimated from the laser linewidth. The consequence is that, in the absence of cavity anisotropies, a well determined direction of linear polarization ψ_0 is only maintained during the time scale of laser coherence.

IV. TRANSVERSE EFFECTS

In this section we study the interplay between transverse effects and polarization dynamics. In the rate equation description we have identified two arbitrary phases θ_0 and ψ_0 , with associated zero eigenvalues. It is generally expected that, when considering transverse effects, long-wavelength fluctuations can destabilize these degrees of freedom through a phase instability. The stability of off-axis laser emission predicted for broad area semiconductor lasers [18] is limited by an instability of the phase θ_0 . We will find here alternative spatiotemporal instabilities associated with the direction of polarization ψ_0 . A natural way to study these aspects would seem to be a generalization of the rate equations to include transverse effects. However, it has been shown that such equations, obtained by adiabatic elimination of the dipole polarization variable, lead to unphysical high-transverse-wave-number instabilities [17]. An alternative approach, which we follow here, is to consider situations close to threshold where an amplitude equation description is appropriate. The dynamical regime covered in this description does not include relaxation oscillations. In terms of the eigenvalues discussed in Sec. III, we will be considering regimes in which $\frac{\gamma_J}{\gamma_{||}} > (\frac{\gamma_J}{\gamma_{||}})_c$ and in which relaxation processes described by the most negative real eigenvalue of (3.7) are considered to be instantaneous. For an ordinary semiconductor laser such a regime is limited to operation very close to threshold, but it is in here where a first clear understanding of the interaction of polarization and transverse degrees of freedom can be obtained. This regime can be easily enlarged by appropriate coatings that produce a better optical cavity reducing the value of the inverse photon lifetime κ .

It is convenient to rescale the system (2.3)–(2.6) to write it in dimensionless form

$$t = \frac{t'}{\gamma_{\perp}}, \quad (x, y) = L(x', y'), \quad F_{\pm} = \frac{i\gamma_{\perp}}{g_0} F'_{\pm},$$

$$P_{\pm} = -\frac{\gamma_{\perp}\kappa}{|g_0|^2} P'_{\pm}, \quad D - \sigma = -\frac{\gamma_{\perp}\kappa}{|g_0|^2} N, \quad d = -\frac{\gamma_{\perp}\kappa}{|g_0|^2} M.$$

(L is the transverse length scale.) Then the dimensionless equations read, with the primes omitted,

$$\partial_t F_{\pm} = -\beta F_{\pm} + \beta P_{\pm} + ia\nabla_{\perp}^2 F_{\pm}, \quad (4.1)$$

$$\partial_t P_{\pm} = -(1 + i\alpha)P_{\pm} + rF_{\pm} - F_{\pm}(N \pm M), \quad (4.2)$$

$$\partial_t N = -bN + (F_{+}^* P_{+} + F_{-}^* P_{-} + c.c.) + d_f \nabla_{\perp}^2 N, \quad (4.3)$$

$$\partial_t M = -hM + (F_{+}^* P_{+} - F_{-}^* P_{-} + c.c.) + d_f \nabla_{\perp}^2 M, \quad (4.4)$$

where

$$\beta = \frac{\kappa}{\gamma_{\perp}}, \quad a = \frac{c^2}{2\nu\gamma_{\perp}L^2}, \quad \alpha = \frac{\omega - \nu}{\gamma_{\perp}},$$

$$b = \frac{\gamma_{\parallel}}{\gamma_{\perp}}, \quad h = \frac{\gamma_J}{\gamma_{\perp}}, \quad d_f = \frac{D_f}{\gamma_{\perp}L^2}, \quad r = \frac{|g_0|^2}{\gamma_{\perp}\kappa}\sigma.$$

The nonlasing solution is given by $F_{\pm} = P_{\pm} = N = M = 0$. As the pumping r is increased, the nonlasing solution loses stability at some threshold. A linear stability analysis of this solution identifies the most unstable modes at threshold. The linearized equations are

$$\partial_t F_{\pm} - ia\nabla_{\perp}^2 F_{\pm} + \beta F_{\pm} - \beta P_{\pm} = 0, \quad (4.5)$$

$$\partial_t P_{\pm} + (1 + i\alpha)P_{\pm} - rF_{\pm} = 0, \quad (4.6)$$

$$N = M = 0. \quad (4.7)$$

We assume that the transverse plane is sufficiently large so that we can neglect boundary conditions and transverse modes form a continuum. Then the solutions for the linear system are of the general form $F_{\pm}, P_{\pm} \propto e^{\lambda t + i\mathbf{k}\cdot\mathbf{x}}$, where \mathbf{k} is the transverse wave vector and $\mathbf{x} \equiv (x, y)$. For a given wave number k , the real part of one of the eigenvalues $\text{Re}(\lambda_1)$ crosses zero from negative as r is increased. Thus $\text{Re}(\lambda_1) = 0$ gives the neutral stability curve $r_0(k)$ [$\text{Re}(\lambda_1) < 0$ for $r < r_0(k)$ and $\text{Re}(\lambda_1) > 0$ for $r > r_0(k)$],

$$r_0(k) = 1 + \left(\frac{\alpha - ak^2}{1 + \beta} \right)^2.$$

Minimizing $r_0(k)$ with respect to k gives the lasing threshold $\min_k r_0(k) = r_0(k_c) = r_c = 1$ with critical wave number k_c and frequency ω_c (which is the imaginary part of λ_1 evaluated at k_c),

$$k_c = \sqrt{\alpha/a}, \quad \omega_c = \alpha. \quad (4.8)$$

The corresponding eigenvectors are

$$(F_{+}, F_{-}, P_{+}, P_{-}, N, M) = e^{i(\mathbf{k}_c \cdot \mathbf{x} - \omega_c t)} \begin{cases} (1, 0, 1, 0, 0, 0) \\ (0, 1, 0, 1, 0, 0). \end{cases}$$

The fact that the most unstable wave numbers are different from zero implies that, close to threshold, the laser will choose to emit off axis. Such off-axis emission occurs in the general model (2.3)–(2.6) for a positive detuning α . For semiconductor laser modeling this detuning is identified with the positive definite α factor [13,14]. Our sim-

plified homogeneously broadened four-level model of the semiconductor laser leads to a constant α factor, which, due to generally smaller transverse intermode spacing, should be a better approximation for transverse effects than for longitudinal multimode problems.

Near threshold any mode with wave number $|\mathbf{k}| \sim |\mathbf{k}_c| = k_c$ can be excited due to the rotational symmetry in the transverse plane. In this paper we will only consider the one transverse dimensional case $\mathbf{k} \sim \pm k_c \hat{\mathbf{x}}$. The amplitude of the most unstable modes can be determined from amplitude equations, an approach of weakly nonlinear analysis that now has become standard [15],

$$(F_{+}, F_{-}, P_{+}, P_{-}, N, M)$$

$$= (1, 0, 1, 0, 0, 0) \left[A_{+} e^{i(k_c x - \omega_c t)} + B_{+} e^{i(-k_c x - \omega_c t)} \right]$$

$$+ (0, 1, 0, 1, 0, 0) \left[A_{-} e^{i(k_c x - \omega_c t)} + B_{-} e^{i(-k_c x - \omega_c t)} \right]$$

$$+ \text{h.o.t.} \quad (4.9)$$

(h.o.t. stands for “higher-order terms”). A_{+} (A_{-} , B_{+} , B_{-}) is the amplitude of the right (left, right, left) circularly polarized, right- (right-, left-, left-) traveling wave. They are assumed to be slowly varying in space and time to take into account a continuum of transverse wave numbers in the small bands centered around $\pm k_c$, which are unstable slightly above threshold. The derivation of the amplitude equations is outlined in the Appendix. By changing variables $t \rightarrow \frac{1+\beta}{\beta}t$, $x \rightarrow \frac{2ak_c}{1+\beta}x$, and $(A_{\pm}, B_{\pm}) \rightarrow \left(\frac{2}{b} + \frac{2}{h}\right)^{-1/2} (A_{\pm}, B_{\pm})$, the amplitude equations can be written

$$(\partial_t + v\partial_x)A_{\pm}$$

$$= \mu A_{\pm} + (1 + i\delta)\partial_x^2 A_{\pm}$$

$$- [|A_{\pm}|^2 + \gamma_1 |B_{\pm}|^2 + \gamma_2 |A_{\mp}|^2 + \gamma_2 |B_{\mp}|^2] A_{\pm}$$

$$- \gamma_3 B_{\pm} B_{\mp}^* A_{\mp}, \quad (4.10)$$

$$(\partial_t - v\partial_x)B_{\pm}$$

$$= \mu B_{\pm} + (1 + i\delta)\partial_x^2 B_{\pm}$$

$$- [|B_{\pm}|^2 + \gamma_1 |A_{\pm}|^2 + \gamma_2 |B_{\mp}|^2 + \gamma_2 |A_{\mp}|^2] B_{\pm}$$

$$- \gamma_3 A_{\pm} A_{\mp}^* B_{\mp}, \quad (4.11)$$

where

$$v = 1 + \frac{1}{\beta}, \quad \mu = r - r_c, \quad \delta = \frac{(1 + \beta)^2}{4\beta a k_c^2} \approx \frac{\gamma_{\perp}}{4\alpha\kappa},$$

$$\gamma_1 = 1 + \frac{(b + 4d_f k_c^2)^{-1} + (h + 4d_f k_c^2)^{-1}}{b^{-1} + h^{-1}}$$

$$= 1 + \frac{(\gamma_{\parallel} + 4\gamma_{\perp} d_f k_c^2)^{-1} + (\gamma_J + 4\gamma_{\perp} d_f k_c^2)^{-1}}{\gamma_{\parallel}^{-1} + \gamma_J^{-1}},$$

$$\gamma_2 = \frac{h - b}{b + h} = \frac{\gamma_J - \gamma_{\parallel}}{\gamma_J + \gamma_{\parallel}} = \frac{\gamma_j}{\gamma_j + \gamma_{\parallel}},$$

$$\gamma_3 = \frac{(b + 4d_f k_c^2)^{-1} - (h + 4d_f k_c^2)^{-1}}{b^{-1} + h^{-1}}$$

$$= \frac{(\gamma_{\parallel} + 4\gamma_{\perp} d_f k_c^2)^{-1} - (\gamma_J + 4\gamma_{\perp} d_f k_c^2)^{-1}}{\gamma_{\parallel}^{-1} + \gamma_J^{-1}}.$$

These equations are a set of coupled complex Ginzburg-

Landau equations (CGLE's) with the important peculiarity that all the coefficients of the nonlinear terms are real. In addition, it is important to note that

$$1 < \gamma_1 \leq 2, \quad 0 < \gamma_2 < 1, \quad \gamma_1 \pm \gamma_3 \geq 1. \quad (4.12)$$

When neglecting carrier diffusion ($D_f = 0$), $\gamma_1 = 2$, and $\gamma_2 = \gamma_3$. In addition, $\gamma_2 > \frac{1}{2}$ for the typical parameter range $\gamma_j > \gamma_{||}$ discussed in Sec. II. We also note that the coupling between right and left circularly polarized amplitudes vanishes as $\gamma_j \rightarrow 0$ and takes a maximum value $\gamma_2 = 1$ as $\gamma_j/\gamma_{||} \rightarrow \infty$. In the reduced description (4.10)–(4.11) the effect of the α factor is taken into account through the parameter δ .

The spatially homogeneous solutions of a general set of four CGLE's, as well as their stability with respect to homogeneous perturbations, have been studied in Ref. [28] in a different context. It turns out that in our range of parameters (4.12) there are only two linearly stable solutions. The first of these solutions is given by

$$A_{\pm} = Q e^{i(\theta_0 \pm \psi_0)}, \quad B_{\pm} = 0, \quad Q^2 = \frac{\mu}{1 + \gamma_2} \quad (4.13)$$

or

$$A_{\pm} = 0, \quad B_{\pm} = Q e^{i(\theta_0 \pm \psi_0)}. \quad (4.14)$$

These solutions correspond to waves traveling in the right or the left direction, linearly polarized in an arbitrary direction ψ_0 . They are the counterpart of the linearly polarized states discussed in Sec. III, but now transverse effects and the α factor lead to a preference for laser emission at a finite transverse wave number k_c . The stability of these solutions is guaranteed by $\gamma_2 < 1$, $\gamma_1 \pm \gamma_3 > 1$.

A second set of linearly stable solutions is given by

$$A_+ = Q e^{i(\theta_0 + \psi_0)}, \quad B_- = Q e^{i(\theta_0 - \psi_0)}, \quad A_- = B_+ = 0 \quad (4.15)$$

or

$$A_- = Q e^{i(\theta_0 - \psi_0)}, \quad B_+ = Q e^{i(\theta_0 + \psi_0)}, \quad A_+ = B_- = 0. \quad (4.16)$$

Their stability is guaranteed by the same conditions $\gamma_2 < 1$ and $\gamma_1 \pm \gamma_3 > 1$. These laser light states correspond to a superposition of traveling waves with the same wave number and opposite circular polarizations. In terms of the Cartesian components F_x and F_y of the vector field \mathbf{F} these states can be visualized as linearly polarized with a periodic direction of polarization $\psi = k_c x + \psi_0$:

$$F_x \propto \cos(k_c x + \psi_0), \quad F_y \propto \sin(k_c x + \psi_0). \quad (4.17)$$

Each Cartesian component of the field is a standing wave (SW). We will not consider these solutions any further since they do not exist when considering any small anisotropy of the laser cavity (see Sec. V).

Among others, there are two additional natural solutions of Eqs. (4.10) and (4.11). The circularly polarized traveling-wave (TW) solutions

$$|A_+| = Q, \quad B_+ = B_- = A_- = 0 \quad (4.18)$$

are unstable for $\gamma_2 < 1$, which is the same reason why they were not considered when neglecting transverse effects. A second unstable solution is the circularly polarized SW

$$|A_+| = |B_+|, \quad A_- = B_- = 0. \quad (4.19)$$

This solution is unstable for $\gamma_1 > 1$, which is the same reason why no stable standing waves are found in broad area lasers when neglecting the polarization degree of freedom [15].

In addition to the homogeneous solutions discussed above, the amplitude equations (4.10) and (4.11) describe slow modulations of the dominant wave vector k_c . General linearly polarized TW solutions are

$$A_{\pm} = Q e^{i(kx + \omega t + \theta_0 \pm \psi_0)}, \quad B_{\pm} = 0, \quad (4.20)$$

$$Q^2 = \frac{\mu - k^2}{1 + \gamma_2}, \quad \omega = -k(v + \delta k). \quad (4.21)$$

Close to threshold, the range of wave numbers k for which these polarized TW are stable is restricted by phase instabilities. A straightforward linear stability analysis of (4.20) is made by writing

$$A_{\pm} = (Q + a_{\pm}) e^{i(kx + \omega t)}, \quad B_{\pm} = b_{\pm}. \quad (4.22)$$

The linear equations for b_{\pm} decouple and perturbations of wave number q are described by two pairs of complex conjugate eigenvalues

$$\lambda_q^1 = \mu - Q^2(\gamma_1 + \gamma_2 + \gamma_3) - q^2 \pm i(q\nu - q^2\delta), \quad (4.23)$$

$$\lambda_q^2 = \mu - Q^2(\gamma_1 + \gamma_2 - \gamma_3) - q^2 \pm i(q\nu - q^2\delta), \quad (4.24)$$

where $b_+ \pm b_-$ are the corresponding eigenvectors. The real part of $\lambda_q^{1,2}$ vanishes at a wave number $k_{1,2}$, so that polarized TW's with wave number k are only stable for $k < k_{1,2}$

$$(k_{1,2})^2 = \frac{\mu(\gamma_1 \pm \gamma_3 - 1)}{\gamma_1 \pm \gamma_3 + \gamma_2}. \quad (4.25)$$

The linear equations for a_{\pm} are most naturally written in terms of the linearly decoupled variables $S = a_+ + a_-$ and $R = a_+ - a_-$,

$$\begin{aligned} \partial_t S &= (1 + i\delta)(-2ik\partial_x S + \partial_x^2 S) \\ &\quad - (\mu - k^2)(S + S^*), \end{aligned} \quad (4.26)$$

$$\begin{aligned} \partial_t R &= (1 + i\delta)(-2ik\partial_x R + \partial_x^2 R) \\ &\quad - (\mu - k^2) \frac{1 - \gamma_2}{1 + \gamma_2} (R + R^*). \end{aligned} \quad (4.27)$$

Both of these equations have an amplitude eigenvalue with a negative real part and a phase eigenvalue that vanishes for zero wave number ($q = 0$) of the perturbation. Explicit expressions for these eigenvalues can be obtained by a straightforward calculation. A more transparent physical approach focuses on long-wavelength fluctuations: We write S and R in terms of real and imaginary

parts as $S = s + i\theta$ and $R = r + i\psi$. As in the analysis of (3.7) and (3.8), the imaginary parts are associated with the global and relative phases of the vector electric field. The real parts are fast relaxing variables that can be adiabatically eliminated. In the long-wavelength limit such elimination leads to phase diffusion equations for the phase variables. The calculation is formally identical for S and R . For S we explicitly find

$$\partial_t s = \partial_x^2 s + 2k\partial_x \theta - \delta\partial_x^2 \theta + 2\delta k\partial_x s - 2(\mu - k^2)s, \quad (4.28)$$

$$\partial_t \theta = \partial_x^2 \theta - 2k\partial_x s + \delta\partial_x^2 s + 2\delta k\partial_x \theta. \quad (4.29)$$

In terms of the Fourier components $s_q e^{-iqx}$ and $\theta_q e^{-iqx}$ of the fluctuations it is obvious that for $q = 0$ there is a zero eigenvalue associated with θ and a real negative eigenvalue associated with the amplitude s . The adiabatic elimination of the amplitude setting $\partial_t s_q = 0$ leads to

$$s_q = \frac{1}{2(\mu - k^2)} \left[\delta q^2 \left(1 - \frac{2k^2}{\mu - k^2} \right) - 2ikq \right] \theta_q + O(q^3). \quad (4.30)$$

Substituting this expression in the equation for $\partial_t \theta_q$, keeping terms up to order q^2 , and going back to x space, a phase equation describing the linear dynamics of long wavelength phase fluctuations is obtained. With a similar analysis for R the phase equations become

$$\partial_t \theta(x, t) = 2k\delta\partial_x \theta + D_\theta \partial_x^2 \theta, \quad (4.31)$$

$$\partial_t \psi(x, t) = 2k\delta\partial_x \psi + D_\psi \partial_x^2 \psi, \quad (4.32)$$

where

$$D_\theta = 1 - \frac{2k^2}{\mu - k^2}, \quad (4.33)$$

$$D_\psi = 1 - 2\frac{(1 + \gamma_2)k^2}{(1 - \gamma_2)(\mu - k^2)}. \quad (4.34)$$

The diffusion coefficient D_θ vanishes at a wave number k_t ,

$$k_t^2 = \frac{\mu}{3}, \quad (4.35)$$

which identifies the conventional Eckhaus instability. TW's with wave number $k > k_t$ are unstable with respect long-wavelength fluctuations of the global phase θ . This stability boundary is the one found in the analysis of broad area lasers when disregarding the polarization degree of freedom and therefore it is independent of the coupling parameter γ_2 . An alternative phase instability associated with the direction of polarization occurs at the wave number k_p for which $D_\psi(k_p) = 0$,

$$k_p^2 = \frac{\mu}{1 + 2\frac{1 + \gamma_2}{1 - \gamma_2}}. \quad (4.36)$$

We have identified four stability boundaries: $k_{1,2}$, which depend on carrier diffusion, and k_t, k_p which are

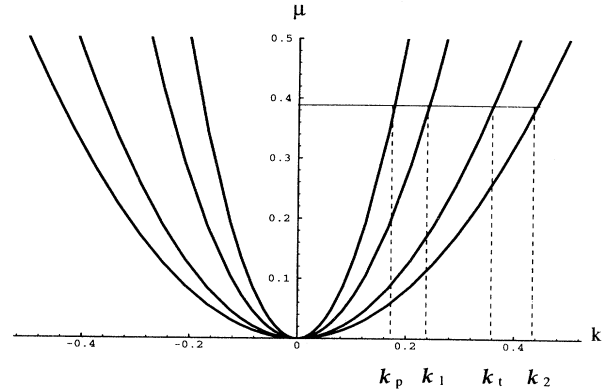


FIG. 4. Stability boundaries for linearly polarized TW's. $D_f = 0$ and $\gamma_2 = 0.7$.

independent of D_f . At least for small values of D_f , the smallest of these wave numbers is k_p , so that the stability range of linearly polarized TW solution is determined by the ψ instability. For $D_f = 0$ we explicitly have

$$k_2^2 = \frac{\mu(1 - \gamma_2)}{2}, \quad k_1^2 = \mu/2 \quad (4.37)$$

and therefore for the physical range of parameter $\gamma_2 > 1/2$,

$$k_p < k_2 < k_t < k_1. \quad (4.38)$$

Figure 4 shows the stability boundaries of linearly polarized TW's in the (μ, k) plane. In the limit of very strong coupling $\gamma_2 \rightarrow 1$ ($\gamma_j \gg \gamma_{j1}$), $k_p \rightarrow 0$ and $k_1 \rightarrow 0$, so that the two inner parabolas in Fig. 4 collapse to zero width. All TW solutions of finite k become unstable and the dominant TW at k_c becomes marginally stable. The polarization phase instability merges in this limit with an amplitude instability of the solution (4.13). This amplitude instability leads to the circularly polarized solution (4.18), which is stable for $\gamma_2 > 1$.

In summary, the rate equation approximation leads to stable linearly polarized laser light with a relaxation time of the polarization perturbations that becomes very large for a large coupling constant γ_j , compared with the difference between the injection current and its threshold value. Transverse effects close to threshold lead to off-axis linearly polarized lasing within a range of wave numbers that shrinks to zero in the limit of very large γ_j . The range of stable wave numbers is determined by a long-wavelength instability of the direction of polarization and it is independent of carrier diffusion.

V. PHASE ANISOTROPIES

In the previous sections we have assumed perfect isotropy of the laser cavity in the transverse x - y plane. Our results indicate that linearly polarized emission is a consequence of the microscopic dynamics of the laser

even under perfect isotropic conditions. However, in most cases, the laser cavity has some anisotropies due to the crystallographic properties of the semiconductor material or due to accidental or intentional cavity built-in anisotropies. Such anisotropies break invariances of the system and lead to preferred directions of linearly polarized emission. For example, it is known for certain gas lasers [3,4,8] that, due to phase anisotropy, there is a switch of polarization direction when changing the cavity detuning through the center of the gain profile. We are particularly interested here in the effect of these anisotropies when transverse effects are important so that we will discuss them in the context of the amplitude equation description. Generally speaking, cavity anisotropies can be classified among amplitude and phase anisotropies and linearly and circular anisotropies [27]. We will consider here a linear phase anisotropy associated with birefringence. Under general symmetry considerations, such phase anisotropy can be modeled by a modification of the set of equations in which the parameter μ is replaced by a matrix defined in the space of the amplitudes (A_+ , A_- , B_+ , B_-),

$$\mu \rightarrow \Gamma = \begin{pmatrix} \mu & i\gamma_p & 0 & 0 \\ i\gamma_p & \mu & 0 & 0 \\ 0 & 0 & \mu & i\gamma_p \\ 0 & 0 & i\gamma_p & \mu \end{pmatrix}, \quad (5.1)$$

where the parameter γ_p measures the strength of the anisotropy. It is arbitrarily taken here that $\gamma_p > 0$. A change of sign of γ_p accounts for the arbitrary change of the x and the y axes.

When $\gamma_p \neq 0$ the SW solutions (4.15) and (4.16) no longer exist. However, there still exist polarized TW solutions (4.20) with a general wave number k , but now with a fixed value of ψ_0 . We find two solutions

$$\cos 2\psi_0 = \pm 1, \quad (5.2)$$

which correspond to linearly x -polarized and y -polarized emission. Both solutions have the same amplitude, which is independent of γ_p ,

$$|A_+|^2 = |A_-|^2 = Q^2 = \frac{\mu - k^2}{1 + \gamma_2}, \quad B_+ = B_- = 0, \quad (5.3)$$

but they have different frequencies

$$\omega_{x,y} = -\nu k - \delta k^2 \pm \gamma_p. \quad (5.4)$$

The stability of these states with preferred direction of linear polarization can be studied in the same way as in Sec. IV, but now for each of the two fixed values of $2\psi_0$:

$$A_{\pm} = (Q + a_{\pm})e^{i\omega t + ikx + i\psi_0}, \quad B_{\pm} = b_{\pm}. \quad (5.5)$$

The equations for a_{\pm} and b_{\pm} are still decoupled and the b_{\pm} perturbations are damped under the same circumstances as for $\gamma_p = 0$. The only modification of the eigenvalues (4.23) and (4.24) is the addition of imaginary contributions $\pm i\gamma_p$. The linear equation for $S = a_+ + a_-$ also decouples and it is independent of γ_p . For

$R = a_+ - a_- = r + i\psi$ we find

$$\partial_t r = \partial_x^2 r + 2\delta k \partial_x r - 2Q^2(1 - \gamma_2)r + 2k \partial_x \psi - \delta \partial_x^2 \psi \pm 2\gamma_p \psi, \quad (5.6)$$

$$\partial_t \psi = -2k \partial_x r + \delta \partial_x^2 r + \partial_x^2 \psi + 2\delta k \partial_x \psi \mp 2\gamma_p r, \quad (5.7)$$

where the upper (lower) sign refers to the x (y) polarized solution. We note that for the dominant wave number $k = 0$ and homogeneous perturbations, the phase dynamics is only driven by perturbations in the relative amplitude of A_+ and A_- .

Taking $r, \psi \sim e^{iqx}$ the phase eigenvalue of (5.6) and (5.7), that is, the one that vanishes for $\gamma_p = 0$ and $q = 0$, is given by

$$\ell = -Q(1 - \gamma_2) - q^2 - 2i\delta k q + [Q^4(1 - \gamma_2)^2 - (\delta q^2 \pm 2\gamma_p)^2 + 4k^2 q^2 + 4ikq(\delta q^2 \pm 2\gamma_p)]^{1/2}. \quad (5.8)$$

Some simple understanding of the implications of (5.8) can be obtained by looking at particularly interesting limits. For the dominant wave vector $k = 0$, the real part of ℓ is negative for any perturbation wave number q . This ensures the linear stability of the x - and the y -polarized traveling waves with wave number k_c , which have equal damping rate at $q = 0$. The fact that the two directions of polarization are stable is a consequence of transverse effects since the freedom to choose a preferred nonvanishing mode k_c compensates for the detuning. Traveling waves of finite k are also stable at $q = 0$. However, for finite k and finite perturbation wave number q one expects a competition between the stabilizing effect at $q = 0$ of the phase anisotropy and the remnant of the ψ instability analyzed in Sec. IV when $\gamma_p = 0$. The result is that destabilization of a TW with a preferred direction of polarization can still occur. Such competition can be described by a damped phase equation associated with the long-wavelength limit $q^2 \ll 1$ of (5.8). If additionally we consider the small phase anisotropy limit $4\gamma_p^2 \ll Q^4(1 - \gamma_2)^2$ we obtain

$$\partial_t \psi(x, t) = \ell_0 + 2k \left(\delta \mp \frac{2\gamma_p}{Q^2(1 - \gamma_2)} \right) \partial_x \psi + D_{\psi}(k, \gamma_p) \partial_x^2 \psi, \quad (5.9)$$

where

$$\ell_0 = -\frac{2\gamma_p^2}{Q^2(1 - \gamma_2)}, \quad (5.10)$$

and

$$D_{\psi}(k, \gamma_p) = 1 \pm \frac{2\delta\gamma_p}{Q^2(1 - \gamma_2)} - \frac{2k^2}{Q^2(1 - \gamma_2)} \left(1 + \frac{6\gamma_p^2}{Q^4(1 - \gamma_2)^2} \right). \quad (5.11)$$

Equation (5.9) accounts for the modification of (4.32) for a small phase anisotropy. The term ℓ_0 gives a phase damping responsible for phase stabilization at $q = 0$. The other terms have different contributions for the x -

and the y -polarized solutions. The vanishing of the diffusion coefficient identifies a modified k_p vector of the ψ instability. To lowest order in γ_p ,

$$k_p^2(\gamma_p) \simeq \frac{\mu \pm 2\delta\gamma_p \frac{1+\gamma_2}{1-\gamma_2}}{1 + 2\frac{1+\gamma_2}{1-\gamma_2}}. \quad (5.12)$$

For $k > k_p(\gamma_p)$ the phase eigenvalue grows with q for long-wavelength fluctuations so that an instability can occur at a finite q . Since $\ell(q=0) < 0$, k_p gives a lower bound for the emergence of the instability. It follows from (5.12) that

$$k_p^x(\gamma_p) > k_p(\gamma_p = 0) > k_p^y(\gamma_p), \quad (5.13)$$

where k_p^x (k_p^y) refers to the x (y) polarized solution. As a consequence, the range of wave numbers for which the x -polarized solution is expected to be stable is increased due to phase anisotropy, while the y -polarized solution has a narrower k -stable range than the x -polarized solution. These general conclusions are illustrated in Fig. 5, where the eigenvalue (5.8) is shown for the same wave numbers k for the x - and the y -polarized solution. For the x -polarized solution, wave numbers $k > k_p(\gamma_p = 0)$ are such that $D_\psi(k, \gamma_p) > 0$, while for the y -polarized solution $D_\psi(k, \gamma_p) < 0$ already for $k = k_p(\gamma_p = 0)$. We also see that the k range of stable TW's is larger for the x -polarized TW than for the y -polarized TW, the lat-

ter being larger but practically coincident with the one for $\gamma_p = 0$. For larger anisotropies the larger value of ℓ_0 tends to compensate for a larger D_ψ so that the k range of stability is not very sensitive to γ_p . In addition, the preference for x -polarized TW solutions of finite k persists.

The main conclusion of the above analysis is that the interplay between the polarization degrees of freedom and transverse effects is such that stabilizing preferred polarization directions for the dominant wave number does not guarantee the stability of polarized TW of nearby wave numbers. This is a consequence of the remnant of the instability of polarization direction for isotropic cavities. On the other hand, also due to transverse effects, there is a discrimination between the two selected directions of polarization in the sense that one of them has a broader range of wave numbers for which polarized TW are stable.

VI. SUMMARY

We have introduced a four-level model for the dynamics of single longitudinal mode, surface-emitting, quantum-well semiconductor lasers that includes the polarization degrees of freedom. The model generally predicts, for a perfectly isotropic cavity, linearly polarized laser emission. The stability and dynamical response to fluctuations of the linearly polarized states is determined by the ratio of time scales associated with spontaneous decay and with spin relaxation processes. For a single transverse mode situation we have analyzed a rate equation approximation that identifies the possibility of polarization relaxation oscillations. Transverse effects have been studied by an amplitude equation description close to threshold, which features a set of four coupled complex Ginzburg-Landau equations. We have found preferred off-axis lasing emission with transverse spatially homogeneous intensity and arbitrary direction of linear polarization, as well as outputs with periodically alternating states of linear polarization in the transverse direction. The stability of the off-axis emission states has been discussed in terms of phase equations. We have found that the range of wave numbers for linearly stable traveling-wave solutions is limited by a phase instability associated with the direction of polarization. We have also considered the effect of anisotropies associated with birefringence, in the framework of the amplitude equation description of transverse effects. Such phase anisotropies select two orthogonal preferred directions of linearly polarized emission. The remnant of the polarization phase instability found for isotropic cavities gives rise to different wave-number stability boundaries for the two directions of polarization.

ACKNOWLEDGMENTS

M.S.M. acknowledges many illuminating insights on polarization laser dynamics from N. B. Abraham. He has also greatly benefited from discussions with Y. Z. Hu. This work has been supported by AFOSR Contract No.

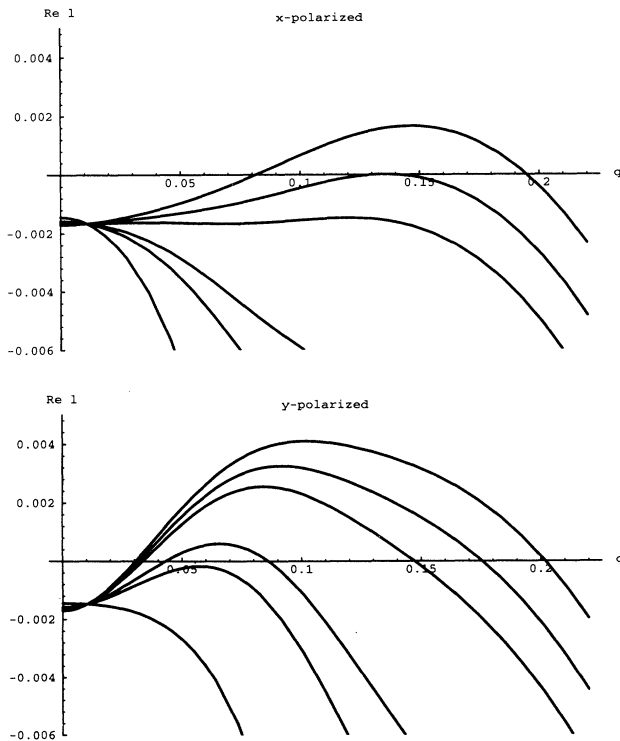


FIG. 5. Real part of the eigenvalue ℓ , Eq. (5.8) for the x - and the y -polarized solutions. Different lines correspond to different wave numbers k . From bottom to top $k = 0$, $k = k_p = 0.127$, $k = 0.140$, $k = 0.160$, $k = 0.165$, and $k = 0.170$. The parameter values are $\mu = 0.2$, $\delta = 2.6$, $\gamma_2 = 0.7$, and $\gamma_p = 0.005$.

F49620-94-1-0144DEF. M.S.M. also acknowledges financial support from Comision Interministerial de Ciencia y Tecnologia (Spain) Project No. TIC93-0744.

APPENDIX

In this appendix we outline the steps for deriving the amplitude equations with a multiple scale method [15]. It is convenient to rewrite Eqs. (4.1)–(4.4) in the compact form

$$[\partial_t + L(\partial_x, r)]\mathbf{v} = N(\mathbf{v}, \mathbf{v}), \quad (\text{A1})$$

where \mathbf{v} denotes the column vector $(F_+, F_-, P_+, P_-, N, M)^T$ (the superscript T means transpose), L is a linear operator, and N a nonlinear one. We expand \mathbf{v} as an asymptotic series in a small parameter ϵ ,

$$\mathbf{v} = \epsilon \mathbf{v}_1 + \epsilon^2 \mathbf{v}_2 + \epsilon^3 \mathbf{v}_3 + \dots, \quad (\text{A2})$$

where

$$\begin{aligned} \mathbf{v}_1 = & (1, 0, 1, 0, 0, 0)^T \left[A_{+1} e^{i(k_c x - \omega_c t)} + B_{+1} e^{i(-k_c x - \omega_c t)} \right] \\ & + (0, 1, 0, 1, 0, 0)^T \left[A_{-1} e^{i(k_c x - \omega_c t)} \right. \\ & \left. + B_{-1} e^{i(-k_c x - \omega_c t)} \right], \quad (\text{A3}) \end{aligned}$$

$$\epsilon^2 = r - r_c. \quad (\text{A4})$$

The small parameter ϵ provides a measure of the distance above threshold. The amplitudes $A_{\pm 1}$ and $B_{\pm 1}$ are assumed to be functions of slowly varying variables

$$X = \epsilon x, \quad T_1 = \epsilon t, \quad T_2 = \epsilon^2 t.$$

Using the chain rule for differentiation, one has the substitution

$$\partial_t \rightarrow \partial_t + \epsilon \partial_{T_1} + \epsilon^2 \partial_{T_2}, \quad \partial_x \rightarrow \partial_x + \epsilon \partial_X, \quad (\text{A5})$$

thus the operator L can be expanded as

$$L = L(\partial_x, r_c) + \epsilon L_1 + \epsilon^2 L_2. \quad (\text{A6})$$

Substituting (A2)–(A6) into (A1) yields a hierarchy of equations for successive orders of ϵ ,

$$\epsilon: [\partial_t + L(\partial_x, r_c)]\mathbf{v}_1 = \mathbf{0}, \quad (\text{A7})$$

$$\begin{aligned} \epsilon^2: [\partial_t + L(\partial_x, r_c)]\mathbf{v}_2 = & -L_1 \mathbf{v}_1 + \mathbf{N}(\mathbf{v}_1, \mathbf{v}_1) \equiv \mathbf{G}_2, \\ & (\text{A8}) \end{aligned}$$

$$\begin{aligned} \epsilon^3: [\partial_t + L(\partial_x, r_c)]\mathbf{v}_3 = & -L_1 \mathbf{v}_2 - L_2 \mathbf{v}_1 + \mathbf{N}(\mathbf{v}_1, \mathbf{v}_2) \\ & + \mathbf{N}(\mathbf{v}_2, \mathbf{v}_1) \equiv \mathbf{G}_3. \quad (\text{A9}) \end{aligned}$$

The ϵ equation is solved by (A3). In order to solve ϵ^2 and ϵ^3 equations, solvability conditions must be satisfied. To apply the solvability condition, we first need to solve a linear problem adjoint to (A7),

$$M^\dagger \mathbf{u} = \mathbf{0}, \quad (\text{A10})$$

where the adjoint operator M^\dagger of $M \equiv \partial_t + L(\partial_x, r_c)$ is defined by the relation

$$\langle \mathbf{u}, M\mathbf{v} \rangle = \langle M^\dagger \mathbf{u}, \mathbf{v} \rangle$$

for vectors \mathbf{u} and \mathbf{v} periodic in x and t with periodicity $2\pi/k_c$ and $2\pi/\omega_c$, respectively (the inner product is defined as $\langle \mathbf{u}, \mathbf{v} \rangle = \int (\mathbf{u}^T)^* \mathbf{v} dx dt$). The explicit form of M^\dagger can be obtained by partial integration and solving (A10) gives four adjoint eigenvectors

$$\begin{aligned} \mathbf{u}_1 &= (1, 0, \beta, 0, 0, 0)^T e^{i(k_c x - \omega_c t)}, \\ \mathbf{u}_2 &= (1, 0, \beta, 0, 0, 0)^T e^{i(-k_c x - \omega_c t)}, \\ \mathbf{u}_3 &= (0, 1, 0, \beta, 0, 0)^T e^{i(k_c x - \omega_c t)}, \\ \mathbf{u}_4 &= (0, 1, 0, \beta, 0, 0)^T e^{i(-k_c x - \omega_c t)}. \end{aligned}$$

At order ϵ^2 , the solvability condition requires

$$\langle \mathbf{u}_i, \mathbf{G}_2 \rangle = 0, \quad i = 1, \dots, 4,$$

which leads to

$$\partial_{T_1} A_{\pm 1} = -\frac{2ak_c}{1+\beta} \partial_X A_{\pm 1}, \quad (\text{A11})$$

$$\partial_{T_1} B_{\pm 1} = \frac{2ak_c}{1+\beta} \partial_X B_{\pm 1}. \quad (\text{A12})$$

Then the solution at this order is given by

$$F_{\pm 2} = 0, \quad (\text{A13})$$

$$P_{\pm 2} = -\partial_{T_1} A_{\pm 1} e^{i(k_c x - \omega_c t)} - \partial_{T_1} B_{\pm 1} e^{i(-k_c x - \omega_c t)}, \quad (\text{A14})$$

$$\begin{aligned} N_2 = & \frac{2}{b} (|A_{+1}|^2 + |B_{+1}|^2 + |A_{-1}|^2 + |B_{-1}|^2) \\ & + \left[\frac{2}{b + 4d_f k_c^2} (A_{+1} B_{+1}^* + A_{-1} B_{-1}^*) e^{2ik_c x} + \text{c.c.} \right], \quad (\text{A15}) \end{aligned}$$

$$\begin{aligned} M_2 = & \frac{2}{h} (|A_{+1}|^2 + |B_{+1}|^2 + |A_{-1}|^2 + |B_{-1}|^2) \\ & + \left[\frac{2}{h + 4d_f k_c^2} (A_{+1} B_{+1}^* - A_{-1} B_{-1}^*) e^{2ik_c x} + \text{c.c.} \right]. \quad (\text{A16}) \end{aligned}$$

The ϵ^3 -order solvability condition is $\langle \mathbf{u}_i, \mathbf{G}_3 \rangle = 0$, $i = 1, \dots, 4$. Making use of (A13)–(A16) we obtain

$$\begin{aligned} \frac{1+\beta}{\beta} \partial_{T_2} A_{\pm 1} = & A_{\pm 1} + \left[\left(\frac{2ak_c}{1+\beta} \right)^2 + i \frac{a}{\beta} \right] \partial_X^2 A_{\pm 1} \\ & - \left(\frac{2}{b} + \frac{2}{h} \right) [(|A_{\pm 1}|^2 + \gamma_1 |B_{\pm 1}|^2 \\ & + \gamma_2 |A_{\mp 1}|^2 + \gamma_2 |B_{\mp 1}|^2) A_{\pm 1} \\ & - \gamma_3 B_{\pm 1} B_{\mp 1}^* A_{\mp 1}], \quad (\text{A17}) \end{aligned}$$

$$\begin{aligned} \frac{1+\beta}{\beta} \partial_{T_2} B_{\pm 1} = & B_{\pm 1} + \left[\left(\frac{2ak_c}{1+\beta} \right)^2 + i \frac{a}{\beta} \right] \partial_X^2 B_{\pm 1} \\ & - \left(\frac{2}{b} + \frac{2}{h} \right) [(|B_{\pm 1}|^2 + \gamma_1 |A_{\pm 1}|^2 \\ & + \gamma_2 |B_{\mp 1}|^2 + \gamma_2 |A_{\mp 1}|^2) B_{\pm 1} \\ & - \gamma_3 A_{\pm 1} A_{\mp 1}^* B_{\mp 1}]. \quad (\text{A18}) \end{aligned}$$

The total time and space derivatives of the amplitudes are given by $\partial_t A_{\pm 1} = \epsilon \partial_{T_1} A_{\pm 1} + \epsilon^2 \partial_{T_2} A_{\pm 1}$ and $\partial_x A_{\pm 1} = \epsilon \partial_X A_{\pm 1}$ (same for $B_{\pm 1}$). Then combining (A11), (A12),

(A17), and (A18) and changing variables $\epsilon A_{\pm 1} = A_{\pm}$ and $\epsilon B_{\pm 1} = B_{\pm}$, we obtain the amplitude equations

$$\begin{aligned} \tau(\partial_t + v_g \partial_x) A_{\pm} &= \epsilon^2 A_{\pm} + \xi^2 (1 + i\delta) \partial_x^2 A_{\pm} \\ &\quad - \left(\frac{2}{b} + \frac{2}{h} \right) [(|A_{\pm}|^2 + \gamma_1 |B_{\pm}|^2 \\ &\quad + \gamma_2 |A_{\mp}|^2 + \gamma_2 |B_{\mp}|^2) A_{\pm} \\ &\quad - \gamma_3 B_{\pm} B_{\mp}^* A_{\mp}], \end{aligned} \quad (\text{A19})$$

$$\begin{aligned} \tau(\partial_t - v_g \partial_x) B_{\pm} &= \epsilon^2 B_{\pm} + \xi^2 (1 + i\delta) \partial_x^2 B_{\pm} \\ &\quad - \left(\frac{2}{b} + \frac{2}{h} \right) [(|B_{\pm}|^2 + \gamma_1 |A_{\pm}|^2 \\ &\quad + \gamma_2 |B_{\mp}|^2 + \gamma_2 |A_{\mp}|^2) B_{\pm} \\ &\quad - \gamma_3 A_{\pm} A_{\mp}^* B_{\mp}], \end{aligned} \quad (\text{A20})$$

where $\tau = 1 + 1/\beta$ and $\xi = 2ak_c/(1 + \beta)$.

-
- [1] G. P. Agrawal and N. K. Dutta, *Long-Wavelength Semiconductor Lasers* (Van Nostrand Reinhold, New York, 1986).
- [2] A. Knorr, R. Binder, E. M. Wright, and S. W. Koch, *Opt. Lett.* **18**, 1538 (1993); R. Indik, A. Knorr, R. Binder, J. V. Moloney, and S. W. Koch, *ibid.* **19**, 966 (1994); A. Uskov, J. Moerk, and J. Mark, *IEEE J. Quantum Electron.* **30**, 1769 (1994).
- [3] D. Polder and W. van Haeringen, *Phys. Lett.* **25A**, 337 (1967); G. Bouwhuis, *ibid.* **27A**, 693 (1968); W. van Haeringen and H. de Lang, *Phys. Rev.* **180**, 624 (1969); H. de Lang, D. Polder, and W. van Haeringen, *Phillips Tech. Rev.* **32**, 190 (1971).
- [4] R. L. Fork and M. Sargeant III, *Phys. Rev.* **139**, A617 (1965); M. Sargeant III, W. E. Lamb, Jr., and R. L. Fork, *ibid.* **164**, 436, 450 (1967).
- [5] D. Lenstra, *Phys. Rep.* **59**, 299 (1980).
- [6] A rather complete list of references is given by M. Matlin, R. Gioggia, N. B. Abraham, P. Glorieux, and T. Crawford, *Opt. Commun.* (to be published), and N. B. Abraham, M. Matlin, and R. Gioggia (unpublished).
- [7] N. B. Abraham, E. Arimondo, and M. San Miguel, *Opt. Comm.* **117**, 344 (1995).
- [8] H. de Lang and G. Bouwhuis, *Phys. Lett.* **19**, 481 (1965).
- [9] F. Koyama, K. Morito, and K. Iga, *IEEE J. Quantum Electron.* **QE-27**, 1410 (1991); M. Shimuzu, T. Mukai-hara, F. Koyam, and K. Iga, *Electron. Lett.* **27**, 1067 (1991); T. Mukai-hara, F. Koyama, and K. Iga, *IEEE Photonics Tech. Lett.* **5**, 133 (1993).
- [10] A. Chavez-Pirson, H. Ando, H. Saito, and H. Kaube, *Appl. Phys. Lett.* **62**, 3082 (1993); K. D. Choquette and R. E. Leibenguth, *IEEE Photonics Tech. Lett.* **6**, 40 (1994); K. D. Choquette, K. L. Lear, R. E. Leibenguth, and M. T. Asom, *Appl. Phys. Lett.* **64**, 2767 (1994).
- [11] C. J. Chang-Hasuain, J. P. Harbison, L. J. Florez, and N. G. Stoffel, *Electron. Lett.* **27**, 163 (1991); Z. George-Pan *et al.*, *Appl. Phys. Lett.* **63**, 2999 (1993); K. D. Choquette, D. A. Richtie, R. E. Leibenguth, *ibid.* **64**, 2062 (1994).
- [12] H. Li, T. Lucas, J. G. McInerney, and R. A. Morgan, *Chaos, Solitons Fractals* **4**, 1619 (1994).
- [13] H. Haug and H. Haken, *Z. Phys.* **204**, 262 (1967); C. H. Henry, *IEEE J. Quantum Electron.* **QE-18**, 259 (1982); M. Osinski and J. Buus, *ibid.* **QE-23**, 9 (1987).
- [14] C. Etrich, P. Mandel, N. B. Abraham, and H. Zeghlache, *IEEE J. Quantum Electron.* **28**, 811 (1992).
- [15] A. C. Newell and J. V. Moloney, *Nonlinear Optics* (Addison-Wesley, Redwood City, CA, 1992).
- [16] P. Ru, J. V. Moloney, and R. Indik, *Phys. Rev. A* **50**, 831 (1994).
- [17] P. K. Jakobsen, J. V. Moloney, A. C. Newell, and R. Indik, *Phys. Rev. A* **45**, 8129 (1992).
- [18] H. Adachihara, O. Hess, E. Abraham, P. Ru, and J. V. Moloney, *J. Opt. Soc. Am. B* **10**, 658 (1993).
- [19] M. San Miguel, *Phys. Rev. Lett.* (to be published); M. San Miguel, Q. Feng, J. V. Moloney, and A.C. Newell, in *Fluctuation Phenomena: Disorder and Nonlinearity*, edited by L. Vazquez (World Scientific, Singapore, 1995).
- [20] *Optical Orientation*, edited by F. Meier and B. P. Zachachrenya (North-Holland, Amsterdam, 1984).
- [21] R. Ferreira and G. Bastard, *Phys. Rev. B* **43**, 9687 (1991).
- [22] M. Z. Maialle, E. A. de Andrada e Silva, and L. J. Sham, *Phys. Rev. B* **47**, 15 776 (1993).
- [23] T. Uenoyama and L. J. Sham, *Phys. Rev. B* **42**, 7114 (1990).
- [24] T. C. Damen, L. Vina, J. E. Cunningham, J. Shah, and L. J. Sham, *Phys. Rev. Lett.* **67**, 3432 (1991); S. Bar-Ad and I. Bar-Joseph, *ibid.* **68**, 349 (1992).
- [25] W. W. Chow, S. W. Koch, and M. Sargeant III, *Semiconductor-Laser Physics* (Springer-Verlag, Berlin, 1994).
- [26] M. Sargent III, M. O. Scully, W. E. Lamb, Jr., *Laser Physics* (Addison-Wesley, Reading, MA, 1974).
- [27] W. Van Haeringen, *Phys. Rev.* **158**, 256 (1967).
- [28] M. Silber and E. Knobloch, *Nonlinearity* **4**, 1063 (1991); M. Silber, H. Riecke, and L. Kramer, *Physica D* **61**, 260 (1992).